ELEKTRIKA

Journal of Electrical Engineering

Dielectric Properties of Polypropylene Blended with Ethylene-Butene Elastomer for High Voltage Applications

N.A. Azrin[1*], **N.A Ahmad**[1*], **K.Y Lau**[1] and **S.N.H Kamarudin**[1]

[1]Institute of High Voltage and High Current (IVAT), Faculty of Electrical Engineering, Universiti Teknologi Malaysia, 81310 UTM Skudai, Johor, Malaysia.

*Corresponding author: nazalia3@live.utm.my, noorazlinda@utm.my

Abstract: In recent years, polypropylene (PP) has been tremendously explored in high voltage cable applications due to its outstanding thermal and electrical properties. Furthermore, PP is an environment-friendly material that can be recycled, thus making it a promising candidate to replace conventional crosslinked polyethylene. However, the stiffness and brittleness of PP need to be further modified so that it can be utilized for practical cable applications. Recently, elastomer blending has been one of the favorable methods used by the industry to modify PP flexibility. Unfortunately, different types of elastomers bring different compatibility in the PP matrix. In this paper, the dielectric performance of PP, when mixed with ethylene-butene elastomer (EBE), was investigated. The thermal behaviors and morphological analysis were identified by using **a** differential scanning calorimeter and scanning electron microscopy, respectively. Meanwhile, the direct current (DC) breakdown strength was set up referring to the ASTM D3755 standard. Based on the findings, EBE shows a certain degree of compatibility with PP, where uniformly distributed spots were observed. Although the addition of EBE slightly degraded the DC breakdown properties of PP, the performance of PP/EBE blends at low elastomer contents is still good enough compared to conventional XLPE.

Keywords: polypropylene, ethylene-butene elastomer, propylene-based elastomer, DC breakdown strength

1. INTRODUCTION

The emergence of crosslinked polyethylene (XLPE) in the early 1960s had a significant impact on the polymer market, particularly for power cable insulation. Until now, XLPE cables have been commonly employed as high voltage cables, especially in high voltage alternating current (HVAC) applications. Nevertheless, the rapid growth of power demand has urged the need for power cable capacity expansion [1]. The voltage and operating temperature of the power cable will increase as the power demand increases. Hence, the future utilization of XLPE as power cable insulation might pose challenges due to its low operating temperature limit (90 °C) [2], [3].

On the other hand, crosslinking byproducts are the drawbacks of the crosslinking process in XLPE's production which are difficult to eliminate. The crosslinking byproducts may harm the operation of cable insulation especially under HVDC conditions. Moreover, the cable waste of XLPE is hard to recycle due to the nature of thermoset behavior in XLPE.

For HVDC applications, the purity of materials is very important. Based on Hosier et. al [4], the proposed insulation materials for HVDC applications would ideally contain no crosslinking impurities, be recyclable, balance mechanical flexibility, and have good dielectric performance and good mechanical integrity at cable operating temperature.

Environmentally friendly materials are the future trend for power equipment evolution especially for high voltage cable applications [1]. Therefore, the study of thermoplastic-based materials such as low-density polyethylene (LDPE), high-density polyethylene (HDPE), and polypropylene (PP) have been tremendously explored in high voltage insulating cable applications [5]. Among them, PP stands out as a promising option for future cable development owing to its outstanding electrical and thermal properties. Besides recyclable advantages, PP has the potential to replace conventional XLPE due to its capabilities to resist high temperatures and withstand high voltages.

Despite its excellent thermal and electrical properties, the practical use of PP for cable insulation is limited due to its stiffness and brittleness. Therefore, PP needs to be modified for it to be further optimized. Several modification methods can be used to improve the performance of PP including nano-doping, chemical grafting, copolymerization, heat treatment, and elastomer blending [6]. Among them, elastomer blending is widely used in industry because the method is simpler and more practical to adjust the properties of the polymer. Yang et. al [7] conducted the electrical and mechanical test of the

PP blend with ethylene-propylene elastomer. The result showed that PP/elastomer blends present simultaneous enhancement in both breakdown strength and tensile properties at 15 % elastomer content. Meanwhile, Zhou et al. [8] reported, that although the incorporation of polyolefin elastomer (POE) in isotactic polypropylene could jeopardize the dielectric properties as compared to pure PP, PP/POE brings significant enhancement in tensile strength, volume resistivity, and thermal behaviors. Based on another scholar, Gao et al. [9] reported that ethylene-octane elastomer produced a "separated spot" and abrupt boundary in the PP matrix, which suggested poor compatibility between PP and elastomer. Therefore, it is believed that the degree of compatibility significantly affects the breakdown strength. The introduction of elastomers may improve and reduce the dielectric properties of pure PP depending on the degree of compatibility. In this paper, the evaluation of PP/EBE blends in terms of thermal, morphological, and DC breakdown strength is discussed.

2. EXPERIMENTAL

2.1 Materials

The primary polymer utilized in this study was a PP homopolymer model Pro 6531 M, purchased from Lotte Chemical Titan. The elastomer acts as a modifier to alter the flexibility of neat PP. The ethylene-butene elastomer (EBE) model Tafmer DF740 was supplied by Mitsui Chemicals Inc. The EBE employed in this research was composed of 1-butene random copolymers synthesized through metallocene catalyst polymerization. Table 1 and Table 2 summarize the specifications of PP and EBE, respectively.

Table 1. Specifications of PP

Specification	Unit	PP
Melt Flow Rate, MFR (230 °C)	g/10 min	3.5
Density	g/cm^3	0.9
Tensile strength at yield	kg/cm^2	360
Elongation at yield	%	10

Table 2. Specifications of EBE

Specification	Unit	EBE
Melt Flow Rate, MFR (230 ° C/2.16 kg)	g/10 min	6.7
Density	g/cm^3	0.87
Ethylene content	wt%	-
Tensile strength at break	MPa	>8
Elongation at break	%	>1000

2.2 Sample Preparation

Primarily, the materials underwent vacuum-drying at 60 °C for 24 hours to ensure the removal of any moisture present. The PP with respective elastomer content was mixed using a Brabender mixer at 180 °C with 50 rpm for 10 minutes. Afterward, the mixture was subjected to melt-pressing using a hydraulic hot press at 180 °C and a load of 2.5 tons. A thin film sample with approximately 100 μm thickness was formed. The proportion of EBE loading in PP blends was changed across different weight percentages. In this paper, 5 wt%, 10 wt%, 20 wt% and 30 wt% of elastomer content was used. The sample indexes are listed in Table 3.

Table 3. Sample indexes

Index	Elastomer type	Elastomer content
PP	-	-
PP/EBE-5	EBE	5 wt%
PP/EBE-10	EBE	10 wt%
PP/EBE-20	EBE	20 wt%
PP/EBE-30	EBE	30 wt%

2.3 Differential Scanning Calorimetry

TA Instrument differential scanning calorimeter (DSC) 25 was used to identify the melting and crystallization behaviors. 5 mg of the sample was sealed with an aluminum pan. Initially, the sample was subjected to a nitrogen environment and heated from 30 ℃ to 250 ℃ at 10 ℃/min heating rate. The purpose of this process is to remove the thermal history of the sample. Then, the secondary melting trace was obtained when the temperature was increased again from 30 ℃ to 250 ℃ at the same heating rate.

The melting temperature, T_m was obtained from the melting trace curve. Then, the crystallinity, X_c was determined based on equation (1) [8].

$$X_c = \frac{\Delta H_m}{Wf \, \Delta H_0} \tag{1}$$

where ΔH_m is a melting enthalpy of the sample, Wf is the weight fraction of the crystallizable materials and ΔH_0 is the enthalpy value associated with the melting of completely crystalline PP (chosen as 209 J/g [8]).

2.4 Morphology

A Hitachi model TM-3000 tabletop scanning electron microscopy (SEM) was used to determine the cross-section morphology of the samples. Before testing, the samples were immersed in liquid nitrogen and fractured. Afterward, a platinum coating was applied to the samples under vacuum conditions to enhance their resolution.

2.5 DC Breakdown Test Set-up

The DC breakdown test was performed using a Baur PGK 110 HB test set. The DC breakdown test was carried out based on the American Society for Testing and Materials (ASTM) D3755 standard. The sample was positioned between two 6.3 mm diameter ball electrodes, and the test cell was filled with silicone oil to prevent flashover. A step-by-step voltage method was applied where 2 kV was injected every 20 seconds. For the reproducibility of data,

fifteen breakdown points were tested for each material. By employing Equation (2), the breakdown strength was obtained.

$$Breakdown\ strength = \frac{Breakdown\ Voltage\ (kV)}{Thickness\ of\ sample\ (mm)} \quad (2)$$

The breakdown data were described by using Weibull distribution analysis. The Weibull plot was generated using the cumulative distribution function of the two-parameter Weibull, represented by Equation (3).

$$P = 1 - exp\left[-\left(\frac{E}{\alpha}\right)^{\beta}\right] \quad (3)$$

where $P(E)$ is a cumulative probability of failure, E is experimental breakdown strength (kV/mm), α is a scale parameter (kV/mm) that represents the breakdown strength at a cumulative failure probability of 63.2% and β is a shape parameter that quantifies the variation of the breakdown data. The larger the β, the smaller the variation of the experimental breakdown values. Figure 1 depicts the schematic diagram of the DC breakdown test setup. The DC breakdown setup consists of a voltage regulator, a transformer, a rectifier, a current-limiting resistor, and a resistive voltage divider.
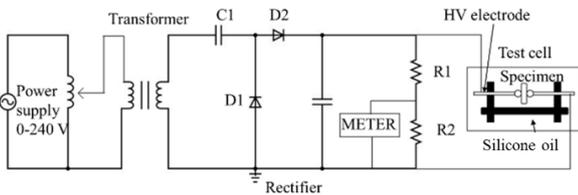

Figure 1. The schematic diagram for the DC breakdown test setup

3. RESULTS AND DISCUSSIONS

3.1 Thermal Properties

Figure 2 and Figure 3 show the melting properties and crystallinity of PP/EBE blends, respectively. The melting peak of PP occurred at 161 ℃, which is in line with the previous work [8]. With the addition of EBE, the thermal properties of pure PP are not significantly affected. Apart from that, the crystallinity of PP/EBE blends decreases with the growth of elastomer, which indicates that the elastomer has restricted the crystallization process [8,10]. The summary of DSC parameters is listed in Table 4.
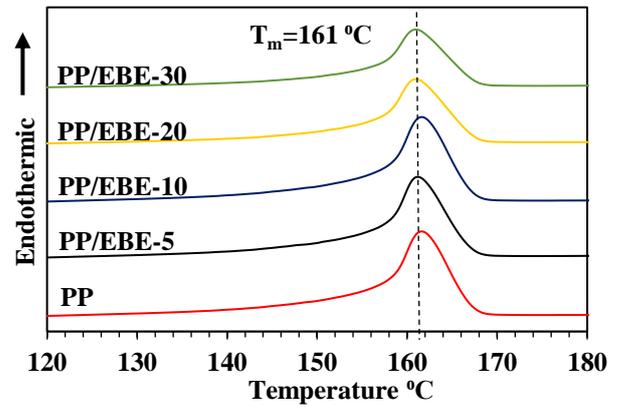

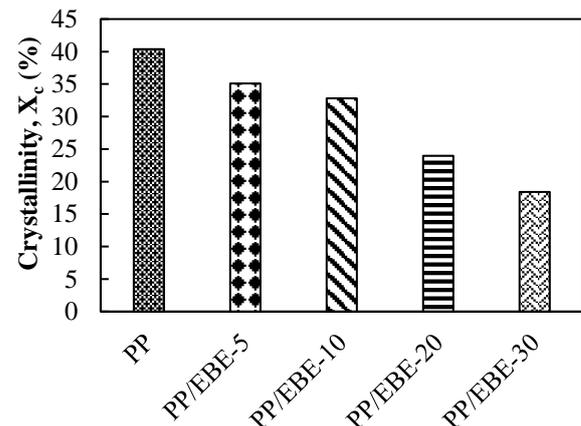Figure 2. DSC melting properties of PP/EBE blends

Figure 3. Crystallinity of PP/EBE blends

Table 4. DSC parameters of PP/EBE blends

Sample	T_m (℃)	Melting Enthalpy, ΔH_m (J/g)	Crystallinity X_c (%)
PP	161.63	84.37	40.37
PP/EBE-5	161.21	77.20	35.09
PP/EBE-10	161.59	76.18	32.08
PP/EBE-20	160.96	62.62	23.97
PP/EBE-30	160.94	54.95	18.40

3.2 Scanning Electron Microscopy (SEM)

The SEM analysis was conducted to identify the dispersion pattern of the elastomer. Figure 4 shows the cross-section morphology for PP and PP/EBE blends. Based on Figure 4(a), the morphology of pure PP is the mono-phase manner, which is affected by fractography characteristics [11-12]. Figure 4(b) depicts the dispersion of EBE in the PP matrix after the incorporation of 5 wt % EBE. Several isolated spots or holes like sea island structures were noticed which indicates the present EBE. The isolated spot is uniformly distributed which suggests that PP and EBE have a certain level of compatibility however not completely compatible. Based on Figure 4 (c)-(e), the isolated spot becomes larger as the EBE loading increases, which indicates the degree of compatibility between PP

and elastomer was reduced significantly.

(a) PP

(b) PP/EBE-5
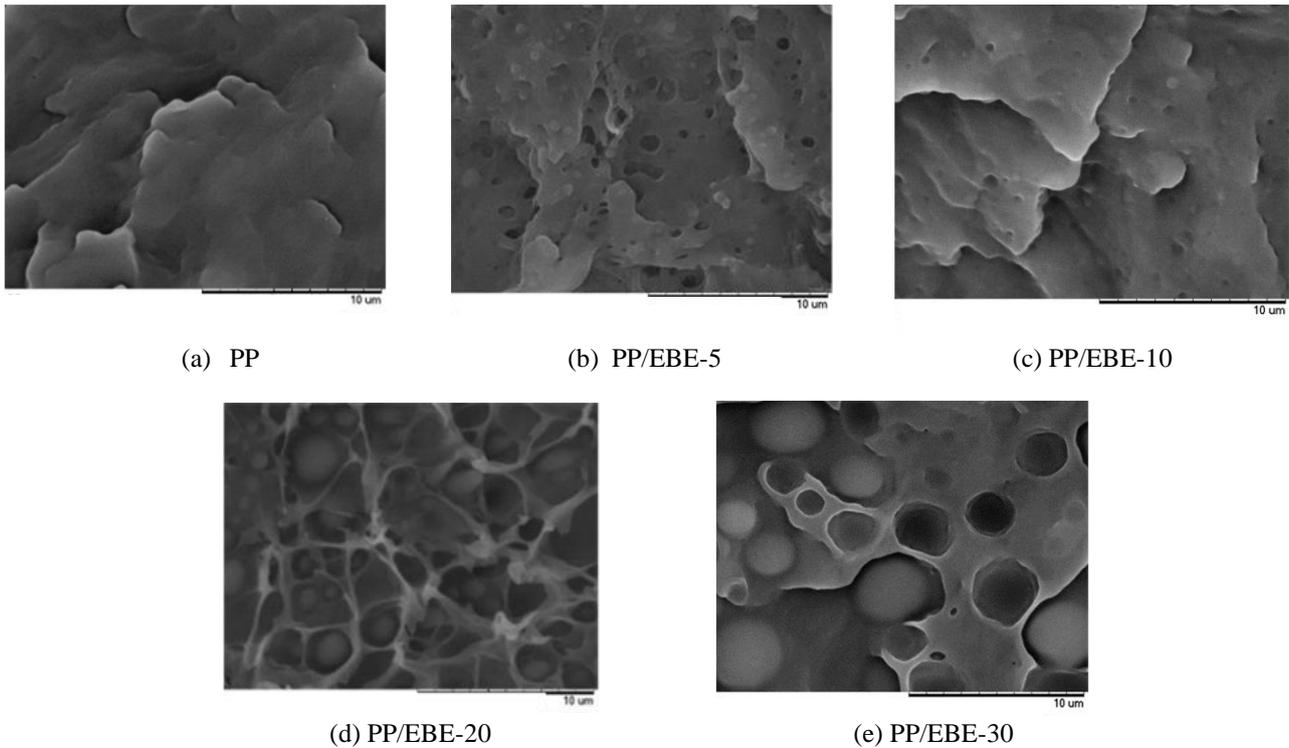

(c) PP/EBE-10

(d) PP/EBE-20

(e) PP/EBE-30

Figure 4. Cross-section morphology of PP and PP/EBE

3.3 DC Breakdown strength

Figure 5 and Table 5 show the Weibull plots and Weibull parameters of DC breakdown properties for the PP/EBE blend. Based on the α value, which represents the breakdown strength, the DC breakdown of pure PP is 353 kV/mm, which is comparable with the result reported by Zhou et. al [8]. When 5 wt % of EBE was added to the PP matrix, it was noticed that the breakdown strength was slightly decreased. As the elastomer content increases, the breakdown strength decreases significantly. Nevertheless, the breakdown strength of PP/EBE blends up to 20 wt% is still comparable with that of the conventional XLPE of 300 kV/mm [13] when considering the uncertainties value. The decreasing trend of DC breakdown can be explained based on several parameters.

Firstly, there is a positive correlation between DC breakdown strength and crystallinity. In essence, crystallinity is indicative of lamella thickness, and the relationship between crystallinity and breakdown strength is significant. Based on the previous study [14], the electrical breakdown strength of the elastomer blend is affected by the crystallinity, and generally, a higher crystallinity is linked to higher breakdown strength. The diminished crystallinity trend (Figure 3) was consistent with the gradual breakdown strength reduction of PP/EBE blends (Figure 5). Therefore, the breakdown strength has been notably impacted by the decrease in crystallinity value.

Besides that, the compatibility of EBE in the PP matrix strongly affected the breakdown strength. The introduction of EBE shows partial compatibility in the PP matrix, which results in a notable decrease in DC breakdown strength. The compatibility of the PP/EBE blend may be influenced by differences in chemical groups, leading to a reduction in interactions between the molecular chains of EBE and PP.

Overall, even though the incorporation of EBE reduced the breakdown strength, the breakdown strength of PP/EBE blends, up to 20 wt%, remains comparable to conventional XLPE. Hence, with the optimal incorporation of elastomer, there is significant potential for PP to serve as a sustainable alternative to XLPE in future cable applications.

4. CONCLUSIONS

This paper reports the findings on thermal, morphological, and DC breakdown strength of PP/EBE blends. The incorporation of EBE does not have a significant impact on the thermal properties of PP. In the morphological aspect, EBE shows a certain degree of compatibility with PP, where uniformly distributed spots were observed. The compatibility reduces with the increased EBE content. The result corresponds with the breakdown strength performance where the breakdown strength of PP/EBE reduces significantly as EBE content increases. Although the introduction of EBE degraded the breakdown strength of PP, the performance of PP/EBE at low elastomer content (below 20 wt%) is still promising to be further explored as it is comparable with the breakdown strength of conventional XLPE.
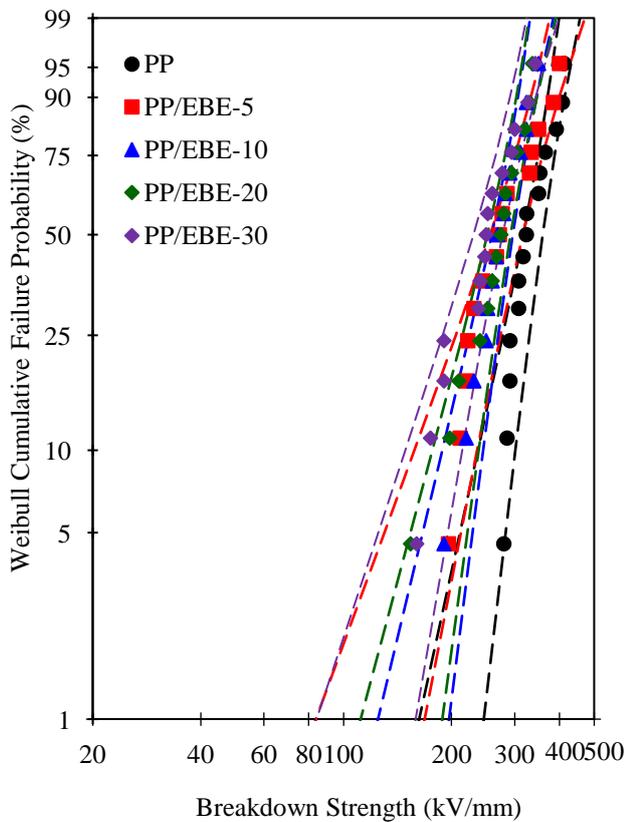
Figure 5. Weibull plots of DC breakdown strength for PP/EBE blends

Table 5. Weibull parameters of DC Breakdown strength

Materials	α (kV/mm)	β
PP	353 ± 21	8 ± 3
PP/EBE-5	307 ± 30	5 ± 2
PP/EBE-10	291 ± 18	7 ± 3
PP/EBE-20	287 ± 19	7 ± 3
PP/EBE-30	271 ± 23	5 ± 3

ACKNOWLEDGMENT

REFERENCES

[1] D. K. Kim *et al.*, "Study on high-temperature and high-voltage insulation characteristics of polypropylene blend with highly packed elastomeric domains for power cable applications," *Polym Test*, vol. 120, no. January, p. 107942, 2023, doi: 10.1016/j.polymertesting.2023.107942.

[2] E. Khouildi, R. Attia, and R. Cherni, "Investigating thermal effect on a cross linked polyethylene power cable," *Indonesian Journal of Electrical Engineering and Computer Science*, vol. 5, no. 1, pp. 33–40, 2017, doi: 10.11591/ijeecs.v5.i1.pp33-40.

[3] S. N. H. Kamarudin, K. Y. Lau, N. A. Ahmad, N. A. Azrin, C. W. Tan, and K. Y. Ching, "Structure and DC Breakdown Properties of Polypropylene/Elastomer Blends," *2023 IEEE 3rd International Conference in Power Engineering Applications: Shaping Sustainability Through Power Engineering Innovation, ICPEA 2023*, pp. 214–216, 2023, doi: 10.1109/ICPEA56918.2023.10093160.

[4] I. L. Hosier, A. S. Vaughan, A. Pye, and G. C. Stevens, "High performance polymer blend systems for HVDC applications," *IEEE Transactions on Dielectrics and Electrical Insulation*, vol. 26, no. 4, pp. 1197–1203, 2019, doi: 10.1109/TDEI.2019.007954.

[5] Y. Zhou, S. Peng, J. Hu, and J. He, "Polymeric insulation materials for HVDC cables: Development, challenges and future perspective," *IEEE Transactions on Dielectrics and Electrical Insulation*, vol. 24, no. 3, pp. 1308–1318, 2017, doi: 10.1109/TDEI.2017.006205.

[6] J. Li, K. Yang, J. Y. Dong, and Z. Jing, "Eco-friendly polypropylene power cable insulation: Present status and perspective," *IET Nanodielectrics*, 2023, doi: 10.1049/nde2.12048.

[7] K. Yang *et al.*, "Enhanced morphology-dependent tensile property and breakdown strength of impact polypropylene copolymer for cable insulation," *Materials*, vol. 13, no. 18, 2020, doi: 10.3390/ma13183935.

[8] Y. Zhou, J. He, J. Hu, X. Huang, and P. Jiang, "Evaluation of polypropylene/polyolefin elastomer blends for potential recyclable HVDC cable insulation applications," *IEEE Transactions on Dielectrics and Electrical Insulation*, vol. 22, no. 2, pp. 673–681, 2015, doi: 10.1109/TDEI.2015.7076762.

[9] Y. Gao, J. Li, G. Chen, T. Han, and B. Du, "Compatibility dependent space charge accumulation behavior of polypropylene/elastomer blend for HVDC cable insulation," *IEEE Transactions on Dielectrics and Electrical Insulation*, vol. 27, no. 3, pp. 947–955, 2020, doi: 10.1109/TDEI.2019.008528.

[10] B. Dang, J. He, J. Hu, and Y. Zhou, "Large improvement in trap level and space charge distribution of polypropylene by enhancing the crystalline-amorphous interface effect in blends," *Polym Int*, vol. 65, no. 4, pp. 371–379, 2016, doi: 10.1002/pi.5063.

[11] Y. Gao, J. Li, Y. Yuan, S. Huang, and B. Du, "Trap distribution and dielectric breakdown of isotactic polypropylene/propylene-based elastomer with improved flexibility for DC cable insulation," *IEEE Access*, vol. 6, pp. 58645–58661, 2018, doi: 10.1109/ACCESS.2018.2874826.

[12] A. Samad, K. Y. Lau, I. A. Khan, A. H. Khoja, M. M. Jaffar, and M. Tahir, "Structure and breakdown property relationship of polyethylene nanocomposites containing laboratory-synthesized alumina, magnesia and magnesium aluminate nanofillers," *Journal of Physics and Chemistry of Solids*, vol. 120, no. January, pp. 140–146, 2018, doi: 10.1016/j.jpcs.2018.04.036.

[13] L. Zhang *et al.*, "Effect of nanoparticle surface modification on breakdown and space charge

behavior of XLPE/SiO2 nanocomposites," *IEEE Transactions on Dielectrics and Electrical Insulation*, vol. 21, no. 4, pp. 1554–1564, 2014, doi: 10.1109/TDEI.2014.004361.

[14] M. Takala *et al.*, "Dielectric properties and partial discharge endurance of polypropylene-silica nanocomposite," *IEEE Transactions on Dielectrics and Electrical Insulation*, vol. 17, no. 4, pp. 1259–1267, 2010, doi: 10.1109/TDEI.2010.5539698.